

Chapter 2

High-Temperature Superconductivity

2.1. Introduction

In 1973, the highest critical temperature of superconductors was only 23K in alloys of niobium and germanium. Thirteen years later, in 1986, Alex Müller and Georg Bednorz [15] at the IBM Zurich Research Laboratory in Switzerland successfully synthesized a new type of superconducting material which consisted of a ceramic oxide of barium, lanthanum, and copper (Ba-La-Cu-O). They observed a dramatic drop in resistivity at 35K, and recognized the possibility of this type of material being a high temperature superconductor. Two months after the publication of Müller and Bednorz's discovery, Shoji Tanaka at the University of Tokyo and Ching-Wu, Paul Chu [16-18] at the University of Houston each independently confirmed the work done in Switzerland. Tanaka's group also determined the structure of the new ceramic superconductor, and found its molecular formula to be $\text{La}_{1.85}\text{Ba}_{0.15}\text{CuO}_4$ [17].

The jewel in the crown of ceramic superconductors, however, was published in March of 1987 when Chu and Wu's groups [18] synthesized $\text{YBa}_2\text{Cu}_3\text{O}_7$, which had a T_c of an incredible 92 K.

Figures 2-1 and 2-2 show the historical development of superconductivity [20]. Note the virtual explosion of papers in 1987 following the discovery of the Ba-La-Cu-O superconducting ceramic by Müller and Bednorz in 1986.

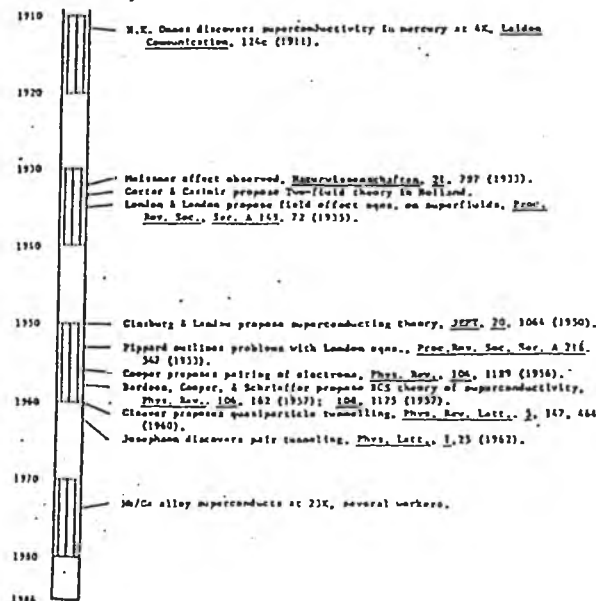


Figure 2-1: Superconductivity Time line from 1900 to 1986. [20]

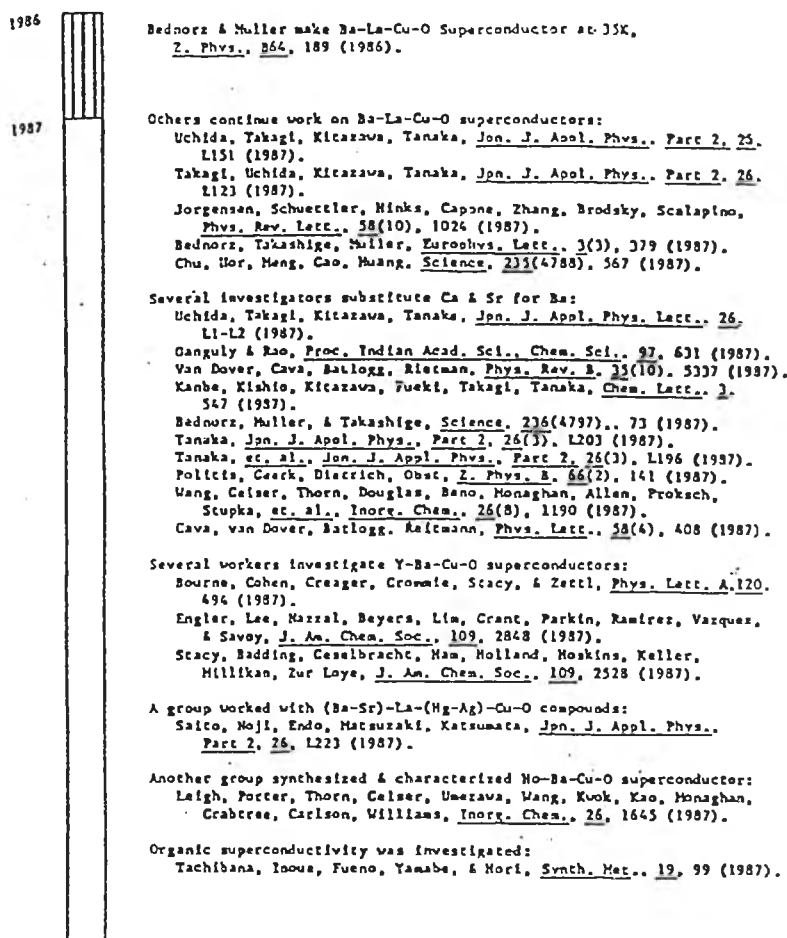


Figure 2-2: Superconductivity Time line for 1986 - 1987. [20]

2.2 Structural and Electronic Properties of the Cuprates

All of the cuprate high- T_c superconductors are quasi-two-dimensional conductors containing one or more CuO_2 layers in each unit cell. The copper-oxygen layer are separated either by intervening Cu-O chains, or by layers containing other metals or metal-oxides (Ba-O, Bi-O, Tl-O, etc.) that serve as the carrier reservoirs. The CuO_2 layers are believed to be the active components of cuprate superconductors, and contain three distinct types of copper-oxygen coordination. All three types of coordination are exhibited by the "214" compounds $(R,R')_{2-x}A_x\text{CuO}_4$, where R and R' are rare earth elements and can be the same element, and $A = \text{Ba}, \text{Sr}, \text{Ca}, \text{Ce},$ or Th acts as a dopant that changes the carrier concentration. Three structural phases T , T' , and T^* are stabilized at room temperature, as illustrated in Fig. 2-3. Each CuO_2 layer consists of an array of CuO_6 octahedra with apical oxygen atoms above and below each copper

site in the T phase, an array of CuO_5 pyramids in the T' phase, and a "checkerboard-like" array of CuO_4 squares in the T' phase. These cuprates exhibit tetragonal symmetry.

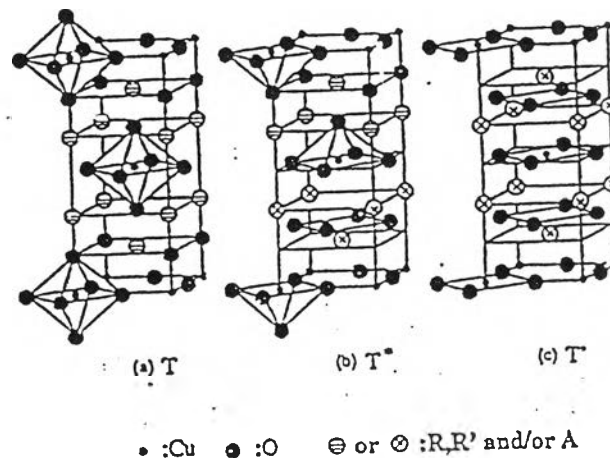


Figure 2-3: The crystal structures of the T , T^* , and T' phase cuprate 214 compounds. R and R' are rare earth elements, while A = Ba, Sr, Ca, Ce, or Th.[55]

Several dozen cuprate superconductors have been discovered since 1986, with T_c 's ranging from zero to 164 K (under pressure). The original cuprate superconductors discovered by Bednorz and Müller [15] were the T phase 214 compound. In this case, the "parent" compound is lanthanum cuprate (La_2CuO_4), which has the KNiO_4 structure. Pure lanthanum cuprate is an antiferromagnetic (AF) insulator containing Cu^{2+} valence states. This compound has the K_2NiO_4 structure (Fig. 3(a)). If one substitutes Ba, Sr, or Ca (Ba^{2+} , etc.) for La (La^{3+}) to create, for example, $\text{La}_{2-x}\text{Ba}_x\text{CuO}_4$ (LaB-214), the Néel temperature T_N for the onset of antiferromagnetism is rapidly suppressed as the hole concentration, which is proportional to x , increases, as shown in the phase diagram in Fig. 2-4. The conductivity increases as the copper ions become mixed valent $\text{Cu}^{2+}/\text{Cu}^{3+}$ and the long-range AF ordering becomes frustrated by the presence of doped holes in the CuO_2 planes. A phase diagram similar to that shown in Fig. 2-4 is obtained for all families of cuprate superconductors. The AF insulating phase consists of in-plane AF ordering of the valence electrons in the CuO_2 layers. As the carrier (eg. hole) concentration is increased by doping the AF parent

compound, the long-range AF ordering is destroyed, although short range AF spin fluctuations persist even in the superconducting state. This phase diagram has been extended in recent years by the observation of a “pseudogap” in optical, angle-resolved photoemission spectroscopy (ARPES), and other measurements. The magnitude of the pseudogap, unlike the T_c , actually goes up with decreasing carrier concentration in the underdoped region, as indicated in Fig.2-4.

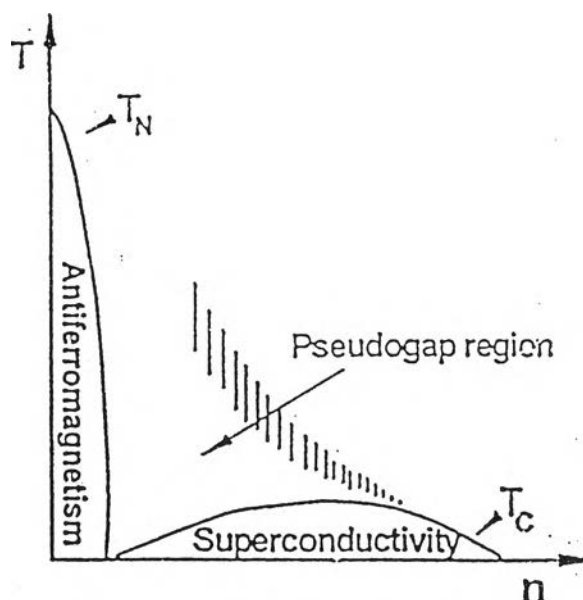


Figure 2-4: The phase diagram of cuprate superconductors, plotting T_N , T_c , etc. as functions of carrier (hole) concentration.[42]

Additional interesting properties have been found in recent neutron scattering studies of $\text{La}_{1.6-x}\text{Nd}_{0.4}\text{Sr}_x\text{CuO}_4$ with $x \sim 1/8$ [45]. The compound has been observed to undergo a succession of transitions: first to the low temperature tetragonal (LTT) structure, then to a charge-ordered state (charge stripes) and finally, at a slightly lower temperature, to a period-doubling magnetically-ordered state. Emery and Kivelson [46] interpret the stripe ordering of hole-rich and hole-poor regions as being driven by frustrated kinetic phase separation. $\text{La}_{1.6-x}\text{Nd}_{0.4}\text{Sr}_x\text{CuO}_4$ with $x \sim 1/8$ does not exhibit bulk superconductivity. However, inelastic neutron scattering experiments [47] have also found evidence for low-energy stripe fluctuations in optimally doped, superconducting $\text{La}_{2-x}\text{Sr}_x\text{CuO}_4$. In particular, the experiments have found peaks at energies as low as a few meV and in essentially the same positions in k -space as in stripe-ordered $\text{La}_{1.6}$.

$x\text{Nd}_{0.4}\text{Sr}_x\text{CuO}_4$. These observations suggest that dynamical stripe correlation may play an essential role in the physics of these materials.

The next family of cuprate superconductors, and the first to exhibit superconductivity above the boiling point of liquid nitrogen, is the so-called "123" (*R*-123) family of compounds $\text{RBa}_2\text{Cu}_3\text{O}_{7-\delta}$, where *R* = Y or any of the rare earth elements except Ce and Tb. The crystal structure of *R*-123 is orthorhombic as shown in Fig. 2-6 and possesses two CuO_2 layers and one CuO chain layer per unit cell. The oxygen stoichiometry is easily varied between O_6 and O_7 due to the loosely bound oxygen atoms in the CuO chains. When the oxygen stoichiometry is less than ~ 6.4 , the CuO chains lose their long range order, and the compound becomes tetragonal and nonsuperconducting. Optimum hole doping (maximum T_c) is attained when the compound is fully oxygenated (i.e. $\delta \sim 0$). The antiferromagnetic insulating phase can be created by reducing the hole concentration by, for example, annealing in a vacuum to remove oxygen or substituting Pr for Y. $\text{PrBa}_2\text{Cu}_3\text{O}_7$ becomes superconducting only when Pr is partially replaced with Ca and, thus far, only in thin film form [48]. Three additional families are: $\text{Bi}_2\text{Sr}_2\text{Ca}_{n-1}\text{Cu}_n\text{O}_{2n+2+\delta}$ [Bi-22(n-1)n]; $\text{Tl}_m\text{Ba}_2\text{Ca}_{n-1}\text{Cu}_n\text{O}_{3-m+3n}$ (with $m = 1, 2$); and $\text{HgBa}_2\text{Ca}_{n-1}\text{Cu}_n\text{O}_{2n+2+\delta}$ [Hg-12(n-1)n] where, in all cases, n ($= 1, 2, 3, \dots$) is the number of CuO_2 planes per unit formula. The structures of the three- CuO_2 -layer thallium- and mercury-based cuprates are shown in Fig. 2-6.

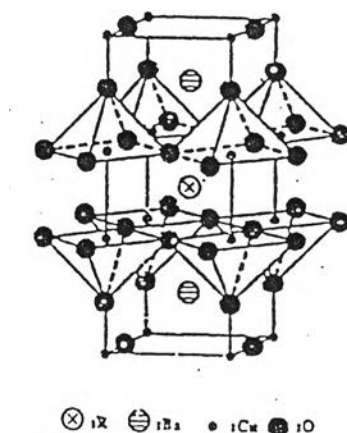


Figure 2-5: The crystal structure of R123 compounds ($R = \text{Y}, \text{La}, \text{etc.}$).[35]

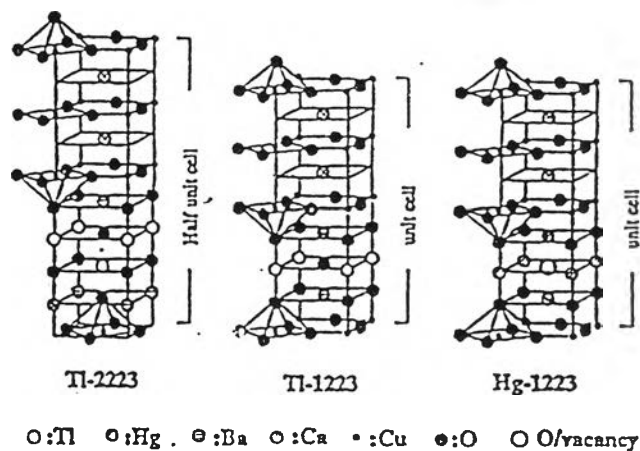


Figure 2-6: The crystal structures of TI and Hg-based cuprates [TI-2223, TI-1223, and Hg-1223] for $n=3$ CuO_2 layers per unit formula.[35]

2.3 The Physics of High-Temperature Superconductivity

A determination of the microscopic origin of high temperature superconductivity is one of the paramount problems of condensed matter physics. This section will attempt to present an overview of what is now known about high T_c superconductivity, within the context of some of the proposed mechanisms.

There is experimental evidence that the remarkable properties of the new metal-oxide superconductors [15-19] result from a pairing of carriers (electrons or holes), as in the case of conventional superconductors. In principle, a sufficiently strong attractive interaction between the carriers would allow a Bose condensation of tightly bound pairs, as originally proposed by Schafroth, Blatt, and Butler[21]. In a conventional BCS-type superconductor, on the other hand, there exist $\sim 10^6$ electrons within the average distance between mates of a single pair [22], so that the pairs do not obey true Bose-Einstein statistics, but the Pauli principle plays an important role. This suggests a classification of theories into (i) BCS pairing, where the pairs form at the transition temperature and (ii) Bose condensation of tightly bound pairs at T_c , where the pairs already exist above the transition temperature.

When the transition temperatures of known superconductors are plotted against the Sommerfeld constant γ , reflecting the density of states $N(0)$ at the Fermi surface, the superconducting materials appear to separate into at least three distinct families, as shown in Fig. 2-7. [23] The heavy fermion superconductors have

anomalously low T_c 's vs. γ as compared with "conventional" superconductors, whereas the new oxide superconductors have T_c 's which are considerably higher than any previous superconductor with comparable γ , and thus appear to comprise a new family of superconductors as pointed out by Batlogg[23].

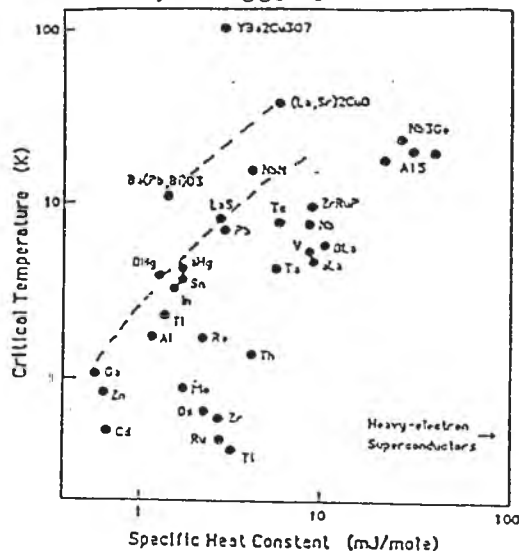


Figure 2-7 : Critical temperature (T_c) versus specific heat constant defined by Sommerfeld constant γ , reflecting the density of states at the Fermi surface. [23]

Extensive measurements of the isotope effect [24-29] in $\text{BaPb}_{1-x}\text{Bi}_x\text{O}_3$, $\text{La}_{2-x}\text{Sr}_x\text{CuO}_4$ (LSCO), and $\text{YBa}_2\text{Cu}_3\text{O}_{7-\delta}$ (YBCO) demonstrate that, for a given compound, T_c scales as $M^{-\alpha}$, where M is the mass of the oxygen isotope and α ranges from about zero in the "123" compounds, with T_c 's of 90-100 K, to $\alpha \sim 0.22$ in $\text{BaPb}_{1-x}\text{Bi}_x\text{O}_3$, with a T_c of ~ 13 K. This indicates that the role of the phonons becomes relatively less important for the higher T_c materials, suggesting that an additional mechanism besides phonon-mediated pairing is largely responsible for superconductivity in the high- T_c "123" compounds. Gurvitch and Fiory (GF, hereafter) [30] have reported on the temperature-dependent resistivities of LSCO and YBCO over the temperature range from T_c to 1100 K. If the electron-phonon interactions were strong, the resistivities would begin to saturate at high temperatures, as is observed in V_3Si . However, the measured resistivities of the new oxide superconductors do not saturate at high temperatures, and the GF results place upper bounds on McMillan's electron-phonon coupling constant [21] of $\lambda \leq 0.1$ and $\lambda \leq 0.3$ for LSCO and YBCO, respectively. Such small values of the electron-phonon coupling constant λ provide

convincing evidence that phonon-mediated pairing cannot be the sole mechanism responsible for high T_c superconductivity.

An important unresolved issue concerns why the T_c 's of the new copper-oxide superconductors are so much higher than those of conventional superconductors. According to the BCS theory [10], in the weak-coupling limit the transition temperature is given by

$$k_B T_c = 1.14 \hbar \omega_c \exp\left(\frac{-1}{N(0)V}\right) \quad (2.1)$$

where V represents an average attractive electron-electron interaction, $N(0)$ is the density states at the Fermi surface, and $\hbar \omega_c$ is a cut-off energy which represents the energy range, measured from the Fermi surface, over which the electron-electron interaction is attractive. This cut-off energy is comparable to the excitations which mediate the pairing. For the case of phonon-mediated pairing, ω_c is comparable to the Debye frequency ω_D . From Eq.(2.1) we can see that there are three ways to increase T_c : (1) increase $N(0)$, (2) increase V , and (3) increase ω_c . In the strong coupling limit, Eq. (2.1) no longer applies, but qualitatively the same trends still hold [33]. A complication is that V and ω_c are not independent for a given pairing mechanism, but are closely related. An increase in V , by strengthening the electron-phonon interaction for example, often occurs at the expense of a reduction in ω_c .

Since it is now known that $N(0)$ is rather low for the high T_c oxide superconductors, the only possibilities, within the BCS framework, are an enhanced attractive interaction V and/or an enhanced cut-off frequency ω_c . The GF experimental results make it highly unlikely that the observed high T_c 's simply result from a large attractive interaction between carriers. It thus appears that the fraction of conducting carriers which participate in the pairing process must be greatly enhanced for the high T_c oxide superconductors, as compared with conventional superconductors.

According to the early theories of high T_c superconductivity proposed by Little [33], Ginzburg [34], and Allender et al. [35], an attractive interaction between carriers can be mediated by the exchange of virtual electron-hole pairs- the so-called "excitonic" mechanism for superconductivity. In order for this mechanism to work, two distinct types of carriers are required- conducting carriers in a metallic region (chain or plane) which

pair to form the superconducting condensate, and polarizable electrons in adjacent regions (side chain or plane) which interact with the metallic carriers to mediate the pairing process. It is possible that the polarizable, nonconducting electrons in the Ba-O planes or the carriers in the Cu-O chains may mediate a pairing between the conducting carriers in the Cu-O planes in the "123" compounds. On the other hand, according to the theory of charge transfer excitation exchange, proposed by Varma et al [36-37], the virtual electronic polarization occurs through the transfer of carriers between the copper and oxygen sites within a Cu-O plane. In this picture the same carriers which mediate the pairing process also participate in forming the superconducting condensate.

The exciton mechanism is predicted to yield a significantly higher T_c than the phonon mechanism because the cut-off energy $\hbar\omega_c$ is expected to be comparable to electronic excitation energies, which are generally much higher than typical Debye energies. Alternatively, one may use the arguments of the isotope effect to arrive at the same conclusion. In the proposed excitonic system the interaction is mediated by the movement of electrons rather than by the much heavier ions of a phonon superconductor. The transition temperature for an excitonic superconductor would thus be scaled up from that of conventional superconductors by a factor of order $(M_{\text{ion}}/m_e)^{1/2}$, if all other parameters were kept constant. The higher energies of the relevant virtual excitations increase the energy range over which the electron-electron interaction is attractive, leading to a higher fraction of paired carriers, and thus a higher T_c .

2.4 Summary of Experimental Results and Theoretical Interpretations

Early positron annihilation experiments of YBCO [38], where the annihilation rates of injected positrons trapped by defects are measured, show a dramatic reduction in the average positron lifetime as the temperature is reduced below the critical temperature. An important conclusion inferred from these studies is that in the superconducting state rather than in the normal state, there is an electronic structure change below T_c . An additional implication is that many, or all, of the conducting carriers in the Fermi sea may be participating in the pairing process, rather than just a narrow

band of states near the Fermi surface. W. Y. Ching et al.[54] have interpreted the positron lifetime results in terms of an excitonic enhanced superconducting mechanism, where excess electrons are available in the superconducting composite state below T_c , but no such electrons exist above T_c .

In the absence of a consensus on the microscopic origin of high T_c superconductivity, a knowledge of the phenomenological Fermi liquid and Ginzburg-Landau (G-L) parameters can help guide in the development (or selection) of a suitable microscopic theory. Bardeen et al. [39] have compiled normal and superconducting parameters of YBCO using estimates based on existing experimental data [40-41], as indicated in Table I. The G-L and Pippard coherence lengths for YBCO, $\zeta_{GL} \sim \zeta_0 \sim 14 \text{ \AA}$, are considerably shorter than those typically found in conventional superconductors. Since the Pippard coherence length ζ_0 is an approximate measure of the average distance between mates of a Cooper pair, when ζ_0 is sufficiently short, a description in terms of real-space pairing and Bose-Einstein condensation becomes viable, unlike the case of conventional superconductivity. On the other hand, the effective penetration length $\lambda_{eff} \sim \lambda_L \sim 1400 \text{ \AA}$ is comparable to the penetration length of an ordinary superconductor. The G-L parameter $\kappa = \lambda_{eff} \sim 100 \text{ \AA}$ is the largest value for any known superconductor. The "123" REBCO (rare earth- $\text{Ba}_2\text{Cu}_3\text{O}_{7-\delta}$) superconductors are thus the most strongly type-II superconductors known. Most importantly, the copper-oxide superconductors are *intrinsically* type-II. In other words they would remain type-II even in the clean limit, where the mean free path length is much longer than the Pippard coherence length, $l \gg \zeta_0$.

(a) Normal State Properties: $\text{YBa}_2\text{Cu}_3\text{O}_{7-\delta}$

Carrier density:	$n = k_F^3 / (3\pi^2) = 9 \times 10^{21} / \text{cm}^3$
Fermi wave vector:	$k_F = 6.5 \times 10^7 \text{ cm}^{-1}$
Density of states: (per spin)	$N(0) = m^* k_F^2 / (2\pi \hbar^2) = 3 \times 10^{14} / \text{cm}^3 \text{ erg}$
Sommerfeld const:	$\gamma = 2\pi^2 k_B^2 N(0) / 3 = 3 \times 10^3 \text{ erg/cm}^3 \text{ K}^2$
Effective mass ratio:	$m^*/m = 9$
Resistivity (90K):	$\rho = 200 \mu\Omega \text{ cm}$
Mean free path (90K):	$\ell = \hbar k_F / (n e^2 \rho) = 17 \text{ \AA}$

(b) Ginzburg-Landau Parameters: $\text{YBa}_2\text{Cu}_3\text{O}_{7-\delta}$

Transition temperature:	$T_c = 90 \text{ K}$
GL penetration depth:	$\lambda_{GL} = 1400 \text{ \AA}$
GL coherence distance:	$\xi_{GL} = 14 \text{ \AA}$
Ratio:	$\kappa \equiv \lambda_{GL} / \xi_{GL} = 100$
Critical fields	$H_c(0) = 12 \text{ kOe}$
$H_{c1} = H_c(0) \ln \kappa / (\sqrt{2} \kappa)$	400 Oe
dH_{c1}/dT	-7 Oe/K
$H_{c2} = \sqrt{2} \kappa H_c$	80 - 320 T

Table 2-1. Normal state and superconducting properties of $\text{YBa}_2\text{Cu}_3\text{O}_{7.8}$ [39]

Studies of the superconducting properties as a function of x in $\text{La}_{2-x}\text{Sr}_x\text{Cu}_4\text{O}_{4.6}$ and as a function of oxygen content in $(\text{RE})\text{Ba}_3\text{Cu}_3\text{O}_{7.8}$ yield information which places constraints on viable theories. An observation inferred from such studies in $\text{La}_{2-x}\text{La}_x\text{CuO}_{4.6}$ by Shafer, Penney, and Olson [42], and subsequently confirmed for $\text{YBa}_{2-x}\text{La}_x\text{Cu}_3\text{O}_{7.8}$ [29], is that the transition temperature T_c scales approximately linearly with the concentration of $[\text{Cu-O}]^+$ complexes. A linear relationship of the form

$$kT_c = \left(\frac{2\pi \hbar^2}{m^*} \right) (n - n_c) \quad (2.2)$$

where n is the concentration of holes per unit area of a single Cu-O plane, is predicted by theories proposing a Bose-Einstein type condensation, such as the resonant valence bond (RVB) theory of Anderson et al. [43-44]. Thus, if the $[\text{Cu-O}]^+$ complexes are identified with mobile holes, then Eq. (2.2) is qualitatively consistent with the observations of Shafer et al [42]. However, when the estimated effective mass of $m^* \sim 9m$ [26] is substituted into Eq.(2.2) , the predicted values of T_c are found to be about an order of magnitude higher than the values experimentally observed for a given hole concentration.

In summary, there are at present a great many more unknowns, including the nature of the pairing mechanism. However, rapid progress is being made towards a detailed understanding of the microscopic origin of high T_c superconductivity.

2.5 Symmetry of Superconducting Order Parameter

The fundamental driving force for high- T_c superconductivity is now widely believed to be the interaction of the doped holes with the antiferromagnetic, or nearly antiferromagnetic, background in the CuO_2 layers. One proposed mechanism for pairing of the holes involves their interaction with antiferromagnetic spin fluctuations [36]. Somewhat surprisingly, a pairing interaction is predicted [37] to be possible even in the presence of a strong on-site Coulomb repulsion and predominantly positive electron-electron (or hole-hole) interaction matrix elements in momentum space. This can be seen by examining the BCS gap equation which is repeated here for convenience:

$$\Delta_k = -\frac{1}{N} \sum_{k'} V_{kk'} \frac{\Delta_{k'}}{2E_{k'}} \tanh(E_{k'}/2T_c). \quad (2.3)$$

In the original BCS theory the matrix elements $V_{kk'}$ were negative, and the gap equation was satisfied (for s-wave superconductors) by taking Δ_k to be have the same sign around the entire Fermi surface. However, although the sign of an s-wave gap function is independent of direction in momentum space, the gap Δ_k actually changes sign when the frequency ω_k (or energy, measured from Fermi surface) exceeds the

phonon frequency., because of the retarded nature of the electron-phonon interaction [37].

The proposed antiferromagnetic spin fluctuation mechanism predicts that the matrix elements $V_{\mathbf{k}\mathbf{k}'}$ will be proportional to the magnetic susceptibility $\chi(\mathbf{k}-\mathbf{k}')$, and will be positive and sharply peaked when $\mathbf{k}-\mathbf{k}' = (\pm\pi/a, \pm\pi/a)$, a being the in-plane lattice parameter (for a tetragonal system). Note, however, that the BCS gap equation (Eq.2.3) can still be satisfied even though the matrix elements $V_{\mathbf{k}\mathbf{k}'}$ are now positive, provided $\Delta_{\mathbf{k}}$ changes sign along the k_y -direction as compared to its sign along the k_x -direction. An important implication is that the gap parameter no longer has s-wave pairing symmetry but, rather, $d_{x^2-y^2}$ pairing state symmetry, as expressed below for a tetragonal system:

$$\Delta(\bar{k}_x, \bar{k}_y) = \Delta_0 [\cos \bar{k}_x a - \cos \bar{k}_y a] \quad (2.4)$$

where Δ_0 is the maximum gap value and a is the in-plane lattice constant. Note that Eq. (2.4) predicts that the gap is positive along the k_x -direction, negative along the k_y -direction, and goes to zero at line nodes along the 45° directions in k -space. Another way of expressing $d_{x^2-y^2}$ pairing symmetry is to use the form $\Delta_{\mathbf{k}} \sim k_x^2 - k_y^2$.

Although $d_{x^2-y^2}$ symmetry had been predicted within the framework of the antiferromagnetic spin fluctuation mechanism, other theories had provided for alternative possibilities. A model combining a phonon mechanism with interlayer coupling [51] had predicted anisotropic s-wave pairing state symmetry, i.e. $\Delta \sim s(k_x^2 + k_y^2)$. An s+id state $\Delta \sim s(k_x^2 + k_y^2) + id(k_x^2 - k_y^2)$ had also been shown to be allowed by symmetry [52], and an anyon state had been shown to correspond to a complex superposition of $d_{x^2-y^2}$ and d_{xy} pairing state symmetry, including any change in sign of the gap states[53]. Because of the heightened interest in determining the nature of the order parameter, a number of experiments were devised to directly probe the superconducting pairing state symmetry, including any change in sign of the gap.